

Dominik Kukla, Andrzej Zagórski, Łukasz Sarniak

Quantitative Evaluation of Eddy Current Signals Generated by Defects in Austenitic Heat Exchanger Tubes

Abstract: The research discussed in the article involved the analysis of impedance characteristics originating from various non-standard defects detected in the material of an austenitic tube. Research-related test results were obtained when scanning a tube made of steel 316, using an internal probe and a Multi-Scan 5800 device. The tests involved the use of the classical ECT vortex current method applied to examine both the tube containing artificial defects, simulating the most common defects in industrial heat exchanger tubular inserts, and reference tubes containing standard defects. The non-standard defects (created artificially) simulated combinations of cracks, pits or other defects formed as a result of exposure to aggressive chemical and mechanical factors present in industrial conditions. The tests involved the scanning of the entire length of the tube at a constant rate. The tests were performed using a transient probe recording electrical impedance changes in a relative mode and in an absolute mode. The interpretation of results related to the non-standard defects was based on a comparison with the results obtained in relation to the standard reference defects. Values obtained in relation to the non-standard defects enabled, among other things, the identification of their volume and position in relation to the measurement probe. In most cases it was not possible to interpret the geometry of a given defect. The foregoing could be achieved using other non-destructive testing techniques.

Keywords: eddy current, diagnostic tests, heat exchangers, austenitic tubes

DOI: [10.17729/ebis.2019.4/6](https://doi.org/10.17729/ebis.2019.4/6)

Introduction

The operation of heat exchangers in industrial conditions entails numerous phenomena including the formation of deposits or defects. One of the reasons for the degradation of (primarily ferritic) materials is corrosion, particularly favoured by such heat exchanger operating

conditions as high temperature, aggressive environment (e.g. acids), stresses (e.g. thermal), condensation and the collection of water at the heat exchanger bottom (lack of discharge valves) or the presence of gaps, deposits, scale or material defects. Another reason for the formation of defects results from erosion, leading

dr inż. Dominik Kukla (PhD (DSc) Eng.) – Institute of Fundamental Technological Research - Polish Academy of Sciences, Warszawa; dr inż. Andrzej Zagórski (PhD (DSc) Eng.); dr inż. Łukasz Sarniak (PhD (DSc) Eng.) – Warsaw University of Technology, Faculty of Materials Science and Engineering, Warszawa;

to the reduction of tube wall thickness and, consequently, perforation. Areas particularly exposed to erosion are various contractions and bends (e.g. curves). In addition, heat exchanger tubes are also exposed to both thermal and fatigue stress components resulting from operation conditions. The above-named stresses should be compensated, yet the local concentration of stresses may initiate a crack. Typical defects formed in heat exchanger tubes are presented in Figure 1 [1].

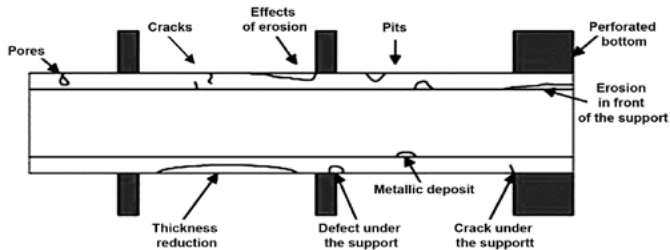


Fig. 1. Typical defects of heat exchanger tubes

Depending on operating conditions, heat exchanger tubes are made of austenitic, ferritic and ferritic-austenitic (duplex) steels as well as nickel, copper and titanium alloys. The safe and failure-free operation of heat exchangers requires the periodic diagnostics of tube condition, performed using non-destructive testing techniques enabling the identification and location of defects having the form of discontinuities, cracks or perforations. Because of the limited access to the surface of heat exchanger tubes, the assessment of their condition is (usually) only possible from the perforated bottom side. For this reason, the most common diagnostic methods (among NDT methods) are based on the use of eddy currents and ultrasounds. The above-named methods enable the assessment of nearly 100% of the tube material volume by inserting a measurement probe inside the tube. Such a solution is the most popular among eddy-current-based testing techniques.

Defects formed in tubular inserts of heat exchangers include both inside and outside wall thickness reduction. The aforesaid thickness

reductions (presented in Figure 2) result in the perforation of the tube wall. For this reason, it is necessary to perform periodic diagnostic tests aimed at the early identification of defects.

Most tube testing techniques involve elec-

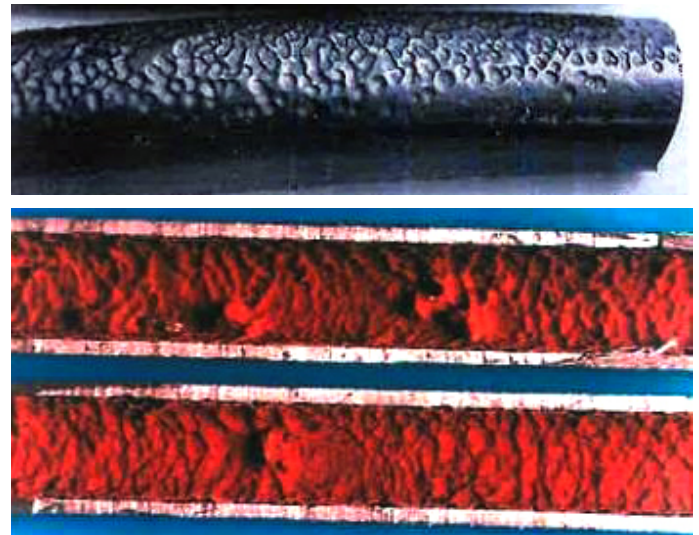


Fig. 2. Internal and external tube wall thickness reduction [3]

tromagnetic methods. The selection of a given diagnostic technique is based on a tube material and its magnetic properties as well as on the potential nature of defects to be detected. The most popular techniques are the following:

- eddy current testing (ECT) – classical method used in tests of tubes made of non-ferromagnetic materials (e.g. austenitic),
- remote field testing (RFT) – method enabling the testing of tubes made of ferromagnetic materials, where the significant value of magnetic permeability restricts the penetration of eddy currents,
- near field testing (NFT) – method enabling the identification of internal defects in tubes provided with aluminium comb-like coating,
- magnetic flux leakage testing (MFLT) – method enabling the measurement of magnetic flux leakage.

Tests of tubes involving the above-presented techniques usually consist in scanning performed inside a tube using a measurement probe. As a result, it is possible to identify discontinuities located on the internal and external tube walls. The proportion of the square of

the probe diameter to the square of the tube diameter should be not less than 0.7. As is the case with most NDT methods, eddy-current testing requires the calibration of a signal using a standard specimen or a reference specimen. This study is focused on the characteristics and analysis of eddy-current signal indications obtained in relation to a designed reference specimen having the form of a tube containing non-standard and complex defects and a standard specimen used commercially during the eddy-current testing technique used when testing austenitic tubes. The analysis of test results aims to facilitate the interpretation of indications in diagnostic practice.

Testing methodology

The test specimens were made of two austenitic steel grades. The specimen containing standard defects was made of steel 304, whereas the reference specimen containing pre-designed non-standard defects was made of steel 316L. Both tubes had an internal diameter of 16 mm. The choice of the material of the specimens used in the eddy-current tests was based on the popularity of steel tubular inserts of heat exchangers and on the availability of the material. The geometry of the defects located on the standard specimen tube is presented in Figure 3. The specimen contained defects in the form of necks (“thickness reductions”) having a depth amounting to 20%, 40% and 60% of the nominal thickness of the tube wall, 10% internal thickness reduction as well as flat-bottomed openings and a pass through opening. To eliminate the signal from supports, a ring (made of the same steel grade

as the tube) simulating support was placed on the standard specimen.

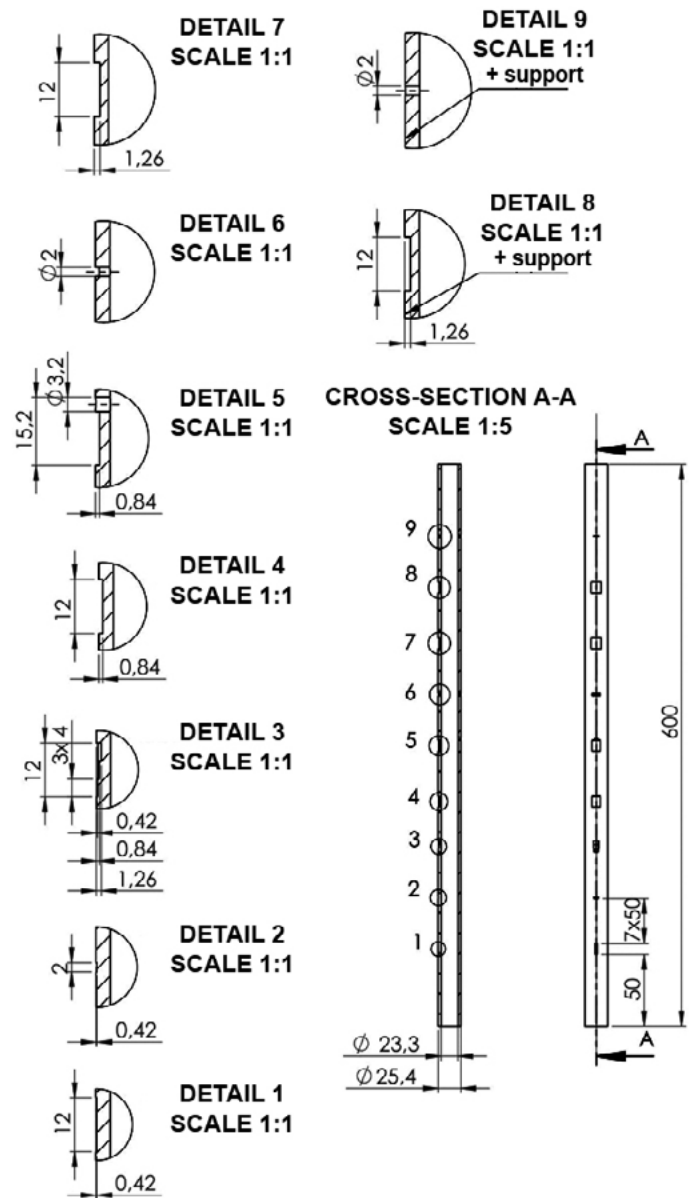


Fig. 4. Production drawing of the tube containing non-standard defects

The calibration of the measurement device (performed using a related standard specimen) was followed by tests of the tube containing non-standard defects, i.e. the combination of discontinuities or material defects, simulating the most “popular” defects found in tubular inserts of heat exchangers. The simulation of actual defects aimed to enable the analysis of indications generated by the above-named defects and the identification of individual discontinuities.

Non-standard defects were the following:

- grooves having a length of 12 mm and depth

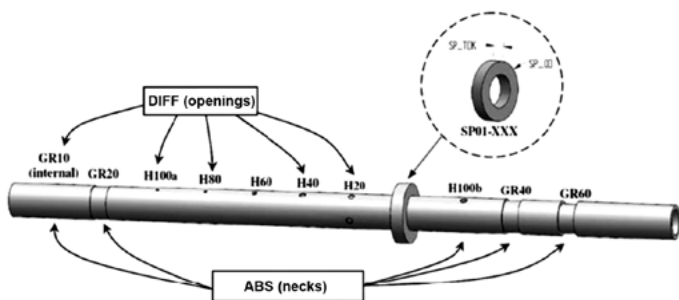


Fig. 3. Standard specimen used in the ECT method [4]

- amounting to 20%, 40% and 60% of the wall thickness,
- groove having a length of 12 mm (3 mm x 4 mm) and depth amounting to 20%, 40% and 60% of the wall thickness,
- groove having a length of 12 mm and depth amounting to 40% of the wall thickness finished with a pass-through opening having a diameter of 3.2 mm,
- pass-through opening having a diameter of 2 mm,
- groove having a length of 12 mm and depth amounting to 60% of the wall thickness with an external circumferential defect.

The geometry of designed non-standard defects is presented in Figure 4. Defects nos. 8 and 9 were tested in presence of a support made of austenitic (a) and ferritic (f) steel.

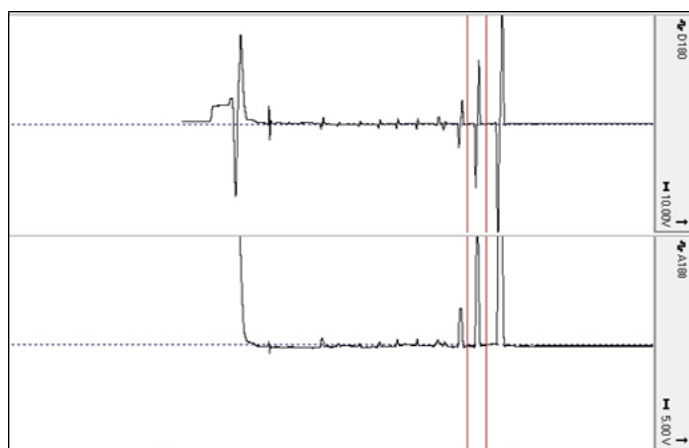


Fig. 5. Dependence of impedance changes in the function of time; the sequence of defects from right to left; the upper diagram shows the course in the differential mode, whereas the lower diagram shows the course in the absolute mode.

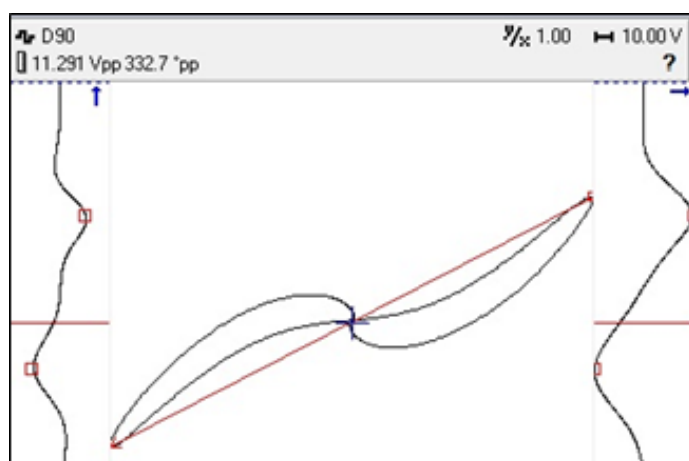


Fig. 6. Exemplary trajectory of changes in voltage and phase angle in relation to the differential probe

The tests were performed using Multi Scan MS5800 eddy current machine (Olympus), a transient probe having a diameter of 14.8 mm (TEA-148-050-N15), a Getac X500G portable computer for industrial applications and a MultiView 6.1Ro software programme. The software programme enabled the visualisation of changes in the impedance of an electric coil in the function of time in the relative and absolute mode (see Figure 5). In addition, after marking a section of a time diagram including a signal generated by one defect, it was possible to obtain the characteristic geometry of the signal along with values of amplitude (V_{pp}) and phase angle (φ_{pp}) (see Figure 6)

To obtain representative and averaged values of amplitude and phase angle, five measurements were performed in relation to each tube. Related values were obtained for 2 measurement channels, i.e. D90 and D180, corresponding to a frequency of excitation current of 24 and 50 kHz respectively. As a result, it was possible to obtain more complete characteristics of defects by using the correlation between the depth of eddy current penetration into the material and the frequency of measurement. In relation to channel D90 and a frequency of approximately 24 kHz, the depth of eddy current penetration into the material of austenitic steel amounted to approximately 4 mm. In turn, in relation to channel D180 and a frequency of approximately 50kHz, the aforesaid depth was restricted within the range of 1.75 mm to 2 mm. In relation to a tube diameter restricted within the range of 2.1 mm to 3.4 mm, channel D90 enabled the detection of 100% of the wall material thickness, whereas channel D180 enabled the detection of approximately 50% of the wall thickness.

Results

Quantitative eddy-current measurement results in relation to the specimen having standard calibration defects (1) are presented as diagrams in Figures 7 and 8. The values of amplitude are

presented in Figure 7, whereas the values of the phase angle in relation to individual defects are presented in Figure 8.

The lowest value of amplitude in relation to frequency D90 (24 kHz) corresponded to defects nos. 5-9, i.e. openings characterised by similar dimensions and geometry. Significantly (even 10 times) higher amplitude values were recorded in relation to the remaining defects (nos. 1-4, no. 10 and 11). The aforesaid values were characterised by significantly more complex geometry and greater volume. In relation to channel D180 (50kHz), a significant increase in amplitude value was recorded. This was because of higher measurement sensitivity of up to 50% of the wall thickness. In turn, a decrease in the value of amplitude was recorded in relation to defect no. 4, simulating a support. The distance between defect no. 4 and the probe was equal to the entire tube wall thickness. As a result, a change in the magnetic field was less detectable in channel D180 (because of the shallower depth of penetration).

In terms of most defects, the values of the phase angle, in relation to channel D90, are restricted within the range of 330° to 360°. As regards defect no. 4 and defects nos. 9-11, the phase angle values differ significantly from the remaining indications. The above-named defects were the support, two pass-through openings and an internal circumferential groove. Based on the aforesaid indications, defects nos. 9-11 could be treated as discontinuities located at the full depth of the wall (pass-through). As regards channel D180, similar phase angle values were also recorded in relation to defects nos. 1-3 and defects nos. 5-8 as well as in relation to defect no. 10. The phase angle values recorded in relation to defect

no. 4 and defects nos. 9-11 were restricted within the range of 335° to 365°. Based on the periodicity of phase angle measurements, the aforesaid values could be treated as close to zero or negative. After the application of the above-presented simplification, points related to defect no. 4 and defects nos. 9-11 will (in a diagram and along with the remaining indications) form a trend indicating the location of a given defect in relation to the measurement probe. The aforesaid location can be defined as the distance between the “centre” of the discontinuity and the probe coil. Subsequent tests were concerned with a tubular specimen containing defects characterised by non-standard geometry (Fig. 4). The measured values of the amplitude of signals and the values of the phase angle are presented in Figures 9 and 10 respectively (using a similar method as that applied in relation to standard specimen no. 1).

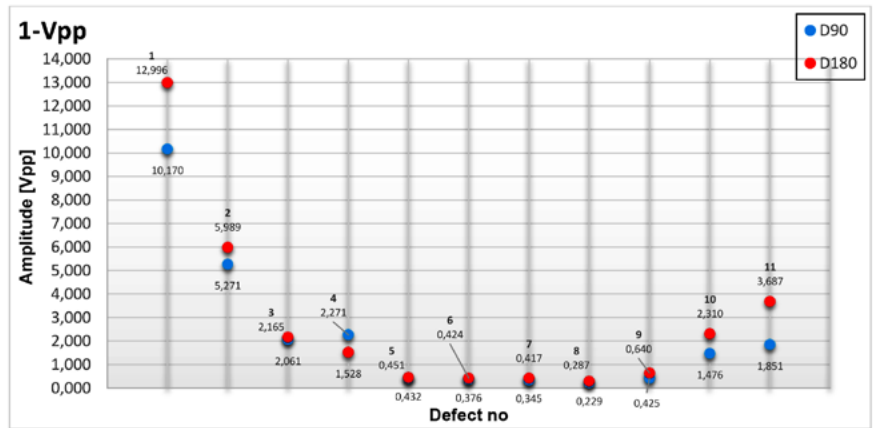


Fig. 7. Values of amplitude in relation to defects in channels D90 and D180 in specimen 1 (standard specimen)

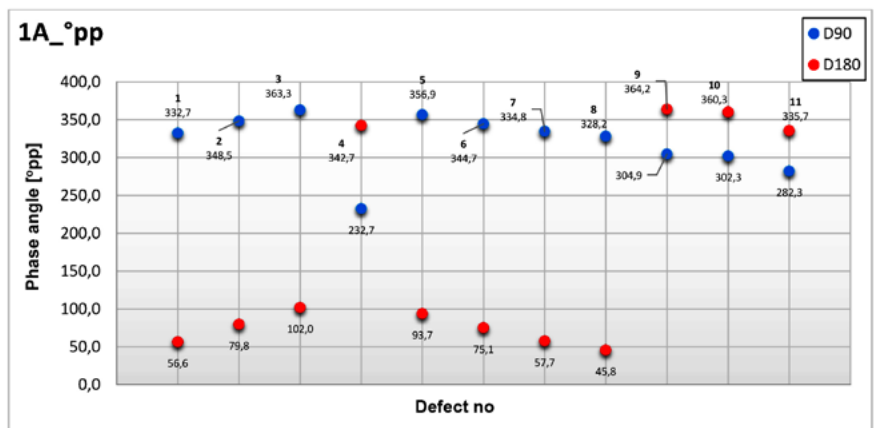


Fig. 8. Phase angle values in relation to defects in channels D90 and D180 in standard specimen 1

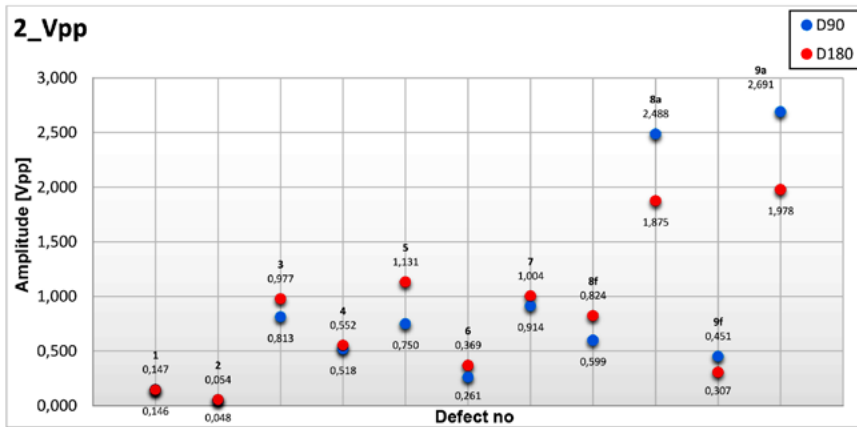


Fig. 9. Values of amplitude in relation to atypical defects in channels D90 and D180 in specimen 2

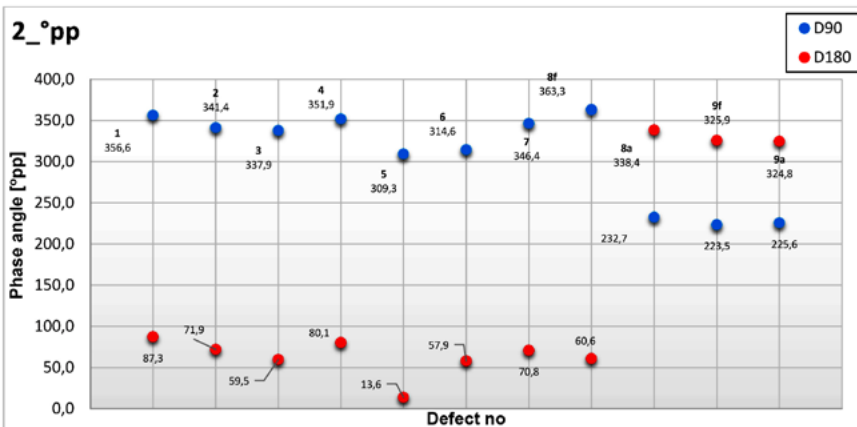


Fig. 10. Phase angle values in relation to atypical defects in channels D90 and D180 in specimen 2

In terms of most defects, higher amplitude values were obtained in relation to channel D180 (because of higher measurement sensitivity). Only in relation to defects no. 8a, 9f and 9a, i.e. in relation to defects located under the austenitic and ferritic support, a higher amplitude value was recorded in relation to channel D90. The foregoing resulted from the increased area of eddy current excitation in the support material. The lowest values were recorded in relation to defect no. 2, which indicated that it had the lowest volume among other defects located in tube no. 2. Slightly higher values were obtained in relation to defect no. 1. The obtained series of amplitude values depends on the volume of individual defects. The significant number of pass-through openings overlaps with the range of eddy current penetration into channel D180. In relation to both channels, i.e. D90 and D180, the values of the phase angle in relation to the

individual non-standard defects of specimen no. 2 (presented in Figure 12) revealed similar trends in the diagram, yet in different ranges of values. Defects characterised by similar geometry and located at a similar depth were characterised by the similar value of the phase angle. As regards channel D90, the above remark applied to pairs of defects no. 1 and 2 and no. 3 and no. 7. When interpreting the location of a given defect in relation to the measurement probe, the key aspect was the location of the “centre” of the defect. Defects nos. 4 and 5 should be characterised by similar values of the phase angle, where the phase angle value related to defect no. 5 should be lower. In addition, the result of defect no. 6 should be lower than that of defect no. 5. The defects were similar in terms of geometry, yet defect no. 6 only included the pass-through opening, without any additional gap. As a result, the “centre” of the discontinuity was not distant from the probe. Because of the overly low value of the phase angle for defect no. 5 in relation to results recorded for all of the discontinuities, the result recorded in relation to the above-named defect confirmed the lack of its coincidence with expected results. Defects no. 7, 8f and 8a were characterised by the same geometry, yet they differed in the material the support was made of or in the presence or absence of the support. The indications of the phase angle in relation to defect no. 8f are the highest among all other defects as the defectoscope interpreted the presence of another material characterised by other properties (carbon steel). The interpretation of the ferromagnetic support as a defect (in this case) is responsible for a significant distance between the defect centre of gravity and the probe. The value of phase

angle in relation to defect no. 8a is significantly lower. The foregoing can be affected by the presence of the support made of the same material as that of the tube. As a result, the relative depth (the external diameter of the ring is regarded as the external surface of the tube wall) of a defect becomes diametrically closer to the probe coil. In relation to the pass-through opening (defect no. 9f and 9a), similar support material-related dependences were observed.

Summary

Using the obtained value of amplitude and phase angle as well as impedance waveform in the function of time in relation to individual discontinuities recorded in two modes (absolute and differential), it is possible to identify the dimensions and the location of a given defect. In addition, in cases of defects characterised by expanded surface, it is possible to qualitatively assess their geometry.

The performed eddy-current measurements made it possible to correlate obtained values with the geometry, location and the volume of standard defects in relation to the measurement probe. The recorded values of amplitude grew along with the increasing volume of a defect. The measured values of a phase angle were directly proportional to the distance between the discontinuity and the measurement probe.

The designed non-standard defects, having a similar geometry or location in relation to the measurement probe as the standard defects, were characterised by similar quantitative and qualitative results. The analysis of the signals would not have been possible without previously formulating conclusions resulting from the tests of the standard defects.

On the basis of obtained results it is possible to identify the parameters of nearly any defect in the material of austenitic tubes as regards

the quantitative evaluation of the amplitude and phase angle of such a defect. The foregoing makes it possible to assess the risk of failure as regards the further operation of a given austenitic tube. However, it is necessary to bear in mind a risk factor when interpreting results connected with numerous factors affecting obtained values of signals, e.g. local changes in the chemical composition, the concentration of stresses or structural changes resulting from, among other things, the preheating of the tube material. To perform complete diagnostics, it is necessary to use complementary NDT techniques, making it possible to confirm information about defects in the structure of the material of an element being tested.

The presence of the support is detectable during the performance of eddy current tests. The above-named presence disturbs the signal, yet, at the same time, it does not exclude the detection of a discontinuity located under the support. The support material is of significance as regards the waveform of voltage characteristics during the test.

The research work was performed within project PBS number ID 246061

References

- [1] <http://www.vikinginspection.co.uk/services/heat-exchangers>.
- [2] Schwartz M.: Four Types of Heat Exchanger Failures. *Plant Engineering*, 1982, no. 12.
- [3] Zbroińska-Szczuchura E., Dobosiewicz J.: Uszkodzenia i diagnostyka wymienników ciepła w elektrociepłowniach. *www.elektroenergetyka.pl*, December 2004, pp. 14-16.
- [4] www.olympusndt.com.